EBioMedicine

Published by THE LANCET

The browning of white adipose tissue and body weight loss in primary hyperparathyroidism

Yang He [a,1], Rui-xin Liu [a,1], Min-ting Zhu [a], Wen-bin Shen [b], Jing Xie [c], Zhi-yin Zhang [a], Na Chen [a], Chang Shan [a], Xing-zhi Guo [a], Yi-de Lu [d], Bei Tao [a], Li-hao Sun [a], Hong-yan Zhao [a], Rui Guo [b], Biao Li [b], Si-min Liu [e], Guang Ning [a,*], Ji-qiu Wang [a,*], Jian-min Liu [a,*]

[a] Department of Endocrine and Metabolic Diseases, Rui-jin Hospital, Shanghai Jiao-tong University School of Medicine, Shanghai Institute of Endocrine and Metabolic Diseases, Shanghai Clinical Center for Endocrine and Metabolic Diseases, Shanghai 200025, China
[b] Department of Nuclear Medicine, Rui-jin Hospital, Shanghai Jiao-tong University School of Medicine, Shanghai 200025, China
[c] Department of Pathology, Rui-jin Hospital, Shanghai Jiao-tong University School of Medicine, Shanghai 200025, China
[d] Clinical Laboratory, Rui-jin Hospital, Shanghai Jiao-tong University School of Medicine, Shanghai 200025, China
[e] Department of Epidemiology and Center for Global Cardiometabolic Health, School of Public Health, Department of Medicine (Endocrinology), The Warren Alpert Medical School, Brown University, Providence, RI, USA

ARTICLE INFO

ABSTRACT

Background: Parathyroid hormone related protein (PTHrP) triggers white adipose tissue (WAT) browning and cachexia in lung cancer mouse models. It remains unknown whether excessive PTH secretion affects WAT browning and to what extent it contributes to body weight change in primary hyperparathyroidism (PHPT).
Methods: Using the adeno-associated virus injection, *Pth* gene over-expressed mice mimicking PHPT were firstly established to observe their WAT browning and body weight alteration. The association between PTH and body weight was investigated in 496 PHPT patients. The adipose browning activities of 20 PHPT and 60 control subjects were measured with PET/CT scanning.
Findings: Elevated plasma PTH triggered adipose tissue browning, leading to increased energy expenditure, reduced fat content, and finally decreased body weight in PHPT mice. Higher circulating PTH levels were associated with lower body weight ($\beta = -0.048$, $P = .0003$) independent of renal function, serum calcium, phosphorus, and albumin levels in PHPT patients. PHPT patients exhibited both higher prevalence of detectable brown/beige adipose tissue (20% *vs* 3.3%, $P = .03$) and increased browning activities (SUV in cervical adipose was 0.77 *vs* 0.49, $P = .02$) compared with control subjects.
Interpretation: Elevated serum PTH drove WAT browning program, which contributed in part to body weight loss in both PHPT mice and patients. These results give insights into the novel pathological effect of PTH and are of importance in understanding the metabolic changes of PHPT.
Fund: This research is supported by the National Key Research and Development Program of China and National Natural Science Foundation of China.

1. Introduction

Parathyroid hormone (PTH), secreted from parathyroid, is a classical hormone acting on bone and kidney for the maintenance of calcium homeostasis. Excessive production of PTH from parathyroid lesion results in primary hyperparathyroidism (PHPT), the third most common endocrine disease, which traditionally characterized by hypercalcemia with bone loss and kidney stone [1].

Energy-storing white adipose tissue (WAT) could be activated to become "beige cells", a recently recognized metabolic process called WAT browning, which can lead to increased energy expenditure and body weight loss [2]. It had recently been reported that cancer-derived PTH related protein (PTHrP) triggered WAT browning and thus causing cachexia in a lung cancer mouse model [3]. Furthermore, ablation of PTH receptor (PTHR), the shared receptor of PTHrP and PTH, in adipose

* Corresponding authors at: Department of Endocrine and Metabolic Diseases, Rui-jin Hospital, Shanghai Jiao-tong University School of Medicine, 197 Rui-jin Er Road, Shanghai 200025, China
E-mail addresses: gning@sibs.ac.cn (G. Ning), wangjq@shsmu.edu.cn (J. Wang), ljm10586@rjh.com.cn (J. Liu).
[1] These two authors contributed equally to this work.

Research in context

Evidence before this study

Primary hyperparathyroidism (PHPT) is a common endocrine disease caused by excessive PTH secretion from parathyroid lesions with classical manifestations of hypercalcemia, bone loss, and kidney stone. It was recently reported that tumor-derived PTHrP, which shares same receptor with PTH, can trigger white adipose tissue browning and cachexia in cancer mouse models. However, it is still unknown whether the overproduction of PTH in PHPT could also drive the adipose browning program and how does it contribute to body weight change.

Added value of this study

In this study, we first built a PHPT mice model which showed activated browning program, resulting in elevated energy expenditure, decreased fat content, and reduced body weight. Next, we identified the browning-triggering effect of PTH by exogenous PTH treatment both *in vitro* and *in vivo.* Furthermore, using data from a relatively large PHPT cohorts, we found that high serum PTH levels were associated with low body weight. Meanwhile, the browning activity was increased in PHPT patients compared to the control ones. Through this series of cellular and animal experiments, together with clinical study in PHPT patients, we report that the overproduction of PTH promotes fat browning program, leading to decreased body weight in mice and humans.

Implications of all the available evidence

Taken together, our findings provid a novel insight into the pathological effect of PTH, a classical calcium-regulating hormone, on adipose tissue browning. Furthermore, our findings are important in comprehensively understanding the metabolic changes of PHPT.

tissue blunted the WAT browning and cachexia in these mice [4], supporting that PTHrP activates the PTHR signal and promotes WAT browning.

PTHrP and PTH are structurally similar and act on the same receptor [5]. However, due to their different binding affinities to PTHR and subsequent signaling pathways [6,7], the physiological and pathological functions of PTH and PTHrP could be inconsistent [5,8–11], giving much uncertainty on the effect of excessive PTH secretion on the browning of WAT in PHPT.

On the other hand, the metabolic disorders in PHPT patients had been widely noticed in the recent decades [12]. Contrary to the hypothesized browning-triggering effect of PTH, large body of study reported that serum PTH levels were positively associated with body weight and body fat mass in humans [13,14]. Furthermore, PHPT patients had higher body weight, elevated body fat content, and higher prevalence of insulin resistance and metabolic syndrome compared with healthy control subjects [15].

To this end, much remains to be known whether the excessive secretion of PTH affects the WAT browning program and how does it contribute to the body weight regulation in PHPT.

In this study, we first successfully established a PHPT mimicked mice model that clearly clarified the pathological effect of PTH in triggering remarkable WAT browning, which led to increased energy expenditure, decreased fat content, and finally reduced body weight. Furthermore, utilizing a large cohort of 496 PHPT patients, we found that higher serum PTH levels were associated with lower body weight independent

of hypercalcemia, serum albumin, and renal function. Importantly, PHPT patients exhibited increased browning activity than control subjects, which might partly explain the body weight loss effect of PTH.

2. Materials and methods

2.1. Materials used in mouse experiments

For chemicals, rat PTH 1–34 and rat PTH 1–84 were purchased from BACHEM (USA). The antibodies against Hsp90 (Cat# 4877, RRID: AB_2233307) and Pparr (Cat# 2443, RRID:AB_823598) were from Cell Signaling Technology. The antibody for Ucp1 was purchased from Alpha Diagnostic (Cat# UCP11-A, RRID: AB_1876090). The antibody for Pgc1a was from Abcam (CAT#ab54481, RRID: AB_881987).

2.2. Adenovirus-associated virus 9 (AAV2/9)-mediated Pth gene overexpression in mice

To establish a mice model with elevated plasma PTH levels, we used the AAV2/9 caudal vein injection to mediate the *Pth* gene overexpression and PTH over-secretion to blood by the virus targeted tissues (AAV2/9 had affinity to organs including heart, muscle, lung, and liver).

The CDS region of mouse *Pth* gene was inserted into the HBAAV-CMV-T2A-GFP vector, under the control of the mouse cytomegalovirus (CMV) promoter. The HBAAV-PTH-T2A-GFP, pAAV-RC and pHepler were co-transfected into AAV-293 cells by using LipoFiterTM transfection reagent (Hanbio, Shanghai, China) to generate the recombinant adeno-associated virus. The AAV was column purified after treatment with Benzonase Nuclease. The empty virus of AAV2/9-GFP was used as a negative control.

2.3. Animal model

Mice were housed on a 12-h light:dark cycle at a constant temperature (22 ± 2 °C) and humidity (50%–70%) with water and a standard rodent chow diet. AAV2/9 was injected *via* the caudal vein into 8 to 9 weeks male C57BL/6 mice using insulin syringes (BD, USA). As the injection of AAV-PTH with 1×10^9 V.g per mouse failed to induce elevated plasma PTH levels and the titer of 1×10^{10} V.g per mouse caused death, 7.5×10^9 V.g per mouse was selected as the final dose. For PTH group, each mouse received a total volume of 100 μl containing 7.5×10^9 V.g AAV-PTH, while each control mouse received a total volume of 100 μl containing 7.5×10^9 V.g AAV-GFP.

2.4. Measurement of fat/lean mass and whole-body metabolism in mice

The fat mass and lean mass of each mouse were measured using an EchoMRI-100H (EchoMRI, Houston, TX). The mice were placed into a Comprehensive Laboratory Animal Monitoring System (CLAMS, Columbus Instruments) to evaluate their whole-body energy metabolism. The oxygen and carbon dioxide data from each mouse were measured every 16 min and were normalized to lean body mass. The activity was measured constantly, and the accumulated values were reported every 16 min. The respiratory exchange ratio (RER) and heat were calculated based on the oxygen and carbon dioxide data and were also normalized to the lean body mass [16].

2.5. Intraperitoneal glucose tolerance test in mice (IPGTT)

The IPGTT was performed three months after virus injection as previously described [17]. Briefly, mice were fasted for 14 h followed by intraperitoneal injection of glucose with a dose of 2 g/kg body weight. The blood glucose of tail vein was measured using a glucose meter (Lifescan, USA) before and 15, 30, 60, 90, and 120 min after glucose injection.

2.6. Insulin tolerance test in mice (ITT)

The ITT was performed three and a half months after virus injection as previously reported [16]. Briefly, mice were fasted for six hours followed by intraperitoneal injection of insulin with a dose of 1 IU/kg body weight. The blood glucose of tail vein was measured using a glucose meter (Lifescan, USA) before and 15, 30, 60, 90, and 120 min after insulin injection.

2.7. Measurement of plasma PTH and serum calcium in mice

EDTA-anticoagulated plasma was prepared for the measurement of intact PTH1–84 using an ELISA assay (Immunotopics, USA). The serum calcium concentration was measured in the clinical laboratory of our hospital using an Arsenazo III assay.

2.8. Femoral BMD measurement

The left femurs of mice were isolated, fixed in 4% paraformaldehyde for 24 h and then maintained in 75% ethanol. The femoral bone mineral density (BMD) was measured by DXA (Discovery Wi, S/N 85170, Hologic, USA). The 5×5 mm area at the distal end of the left femur was selected as the representative area for the analysis of BMD.

2.9. Histology and immune-histology of adipose tissue in mice

Adipose tissue was isolated, fixed in 4% paraformaldehyde, embedded in paraffin and sectioned at 5 μm for HE staining and Ucp1 immuno-histochemical staining (Ucp1 antibody diluted in PBS at 1:250) [16].

2.10. Primary cell culture and differentiation

The Stromal Vascular Fraction (SVF) of the inguinal fat pads was isolated from 4 to 6 weeks male C57BL/6 mice, as described previously [16]. In brief, the inguinal fat pads were isolated, cut into pieces, and digested in Type II Collagenase (Sigma, USA) at 37 °C for 30 min followed by quenching with complete medium. The suspended samples were filtrated using a 40-μm strainer (BD, USA) and plated on the culture dish with adipocyte culture medium, which contained DMEM/F12 and 10% FBS. These primary adipose cells were differentiated into beige adipocyte in a cocktail containing 5 μg/ml insulin, 1 μM dexamethasone, 1 μM rosiglitazone, and 0.5 mM IBMX for the first two days. At day three and day five, the medium was changed to containing 5 μg/ml insulin and 1 μM rosiglitazone. Beginning on day seven, the cells were cultured only in the adipocyte culture medium. The cells were harvested on day eight. For the intervention study, the cells were treated with rat PTH 1–84 or vehicle for two hours, four hours, or 24 h before harvesting on day eight.

2.11. Oxygen consumption rate (OCR) measurement in differentiated SVFs

SVFs from inguinal fat pads were isolated as described above and were seeded in an XF24 V28 microplate (Seahorse Bioscience) coated with poly-L-lysine (Sigma), followed by differentiation into beige adipocytes in the cocktail as described above with treatment of rat PTH1–84 or Vehicle for five days. Subsequently, the OCR was measured as previously described [18] using an XF24 analyzer (Seahorse Bioscience) according to manufacturer's instructions. Briefly, the culture medium of the cells was changed to Seahorse XF base medium with 25 mM D-glucose, 2 mM sodium pyruvate, and 2 mM LG and incubated at 37 °C in a non-CO_2 incubator (Seahorse Bioscience) for one hour. Respiratory inhibitors (Seahorse Bioscience, 103,015–100) including 1 mg/ml oligomycin, 1.5 mM FCCP, 0.5 mM antimycin A, and 0.5 mg/ml rotenone were loaded into the injection port in sequence and to detect the base respiration, uncoupled respiration, maximal respiration, and non-

mitochondrial respiration, respectively. The final OCR results were standardized to the protein concentration.

2.12. Western blot

Total protein from adipose tissue was isolated using RIPA (Biocolors, Shanghai, China) and a Protease Inhibitor Cocktail (Sigma, USA). The concentration of protein was measured using a BCA protein assay kit (Thermo Scientific Pierce, USA) and 15–20 μg of the protein lysates were separated in each SDS-PAGE lane. The separated proteins were then transferred to a PVDF membrane (Millipore, USA) under 100 V for 120 min at 4 °C, and the membrane was blocked in 5% BSA at room temperature for one hour, followed by an overnight incubation in primary antibody at 4 °C. The next day, TBS-T containing 5% BSA was used for incubation of secondary antibody at room temperature for one hour. The results were visualized using a charge-coupled device (CCD) camera system (ImageQuant LAS 4000, GE, Milwaukee, WT) using Enhanced chemiluminescence (ECL) western blotting substrates (Millipore, USA).

2.13. Reverse transcription and qPCR

Total RNA was extracted from cultured cells or frozen adipose tissue using TRIzol reagent (Invitrogen, USA). The absorbance ratio at 260/280 nm and the RNA concentration of all samples were checked using a Nano-Drop ND-2000 spectrophotometer (Thermo Scientific, USA). The reverse transcription was performed using PrimeScriptTM Reverse Transcript Master Mix (TaKaRa, Japan), followed by the qPCR conducted using a QuantStudio™Dx Real-Time PCR Instrument (Applied Biosystems, USA). The comparative CT method was used to evaluate the relative mRNA levels and 36b4 was used as the reference. The primers *Ucp1*, F: AGGCTTCCAGTACCATTAGGT, R:CTGAGTGAGGCAAA GCTGATTT; *Pgc1a*, F: AGCCGTGACACTGACAACGAG, R:GCTGCATGGTT CTGAGTGCT AAG; *Cidea*, F:TGCTCTTCTGTATCGCCCAGT, R:GCCGTGTTA AGGAATCT GCTG; *Pparr*, F:GCATGGTGCCTTCGCTGA, R:TGGCATCTCTG TGTCAACCA TG; *Dio2*, F:AATTATGCCT CGGAGAAGACCG, R: GGCAGT TGCCTAGTGAA AGGT; *36b4*, F: GAAACTGCTGCCTCACATCCG, R:GCTG GCACAGTGACCTC ACACG; *Prdm16*, F:CCACCAGCGAGGACTTCAC, R: GGAGGACTCTCGTAGC TCGAA.

2.14. Patient population and selection

All data from 597 patients with PHPT continuously admitted to Rui-jin hospital, Shanghai Jiao-tong University School of Medicine from January 2000 to December 2015 were retrospectively reviewed. A total of 496 PHPT patients were selected for this study based on the following criteria: 1) age ≥ 18 years, 2) with complete records for serum PTH, height, and body weight.

We measured height and weight at the time of admission under standardized conditions. Body mass Index (BMI) was calculated as weight/height^2. Serum levels of intact PTH were measured using an intact immunoradiometric assay (Abbott, Architect i2000SR, USA). The following clinical data were recorded for further analysis: 1) demographic data, including sex and age; 2) biochemical index on admission, including serum calcium, phosphorus, 25-hydroxy vitamin D (25(OH) D), serum creatinine, and albumin; 3) pathological diagnosis.

2.15. PET/CT scan and analysis in PHPT patients

The PET/CT scan images from 20 PHPT patients were retrospectively reviewed. Sixty patients who received a PET/CT scan in Rui-jin hospital who met the following criteria were selected as healthy control subjects: 1) sample size: matched with PHPT patients at a ratio of 3:1; 2) matched with PHPT patients for sex, age (5-year intervals), BMI (3 kg/m^2 intervals) and outdoor temperature (5 °C intervals) on the scanning day; 3) without diabetes; 4) without cancer, hyperthyroidism,
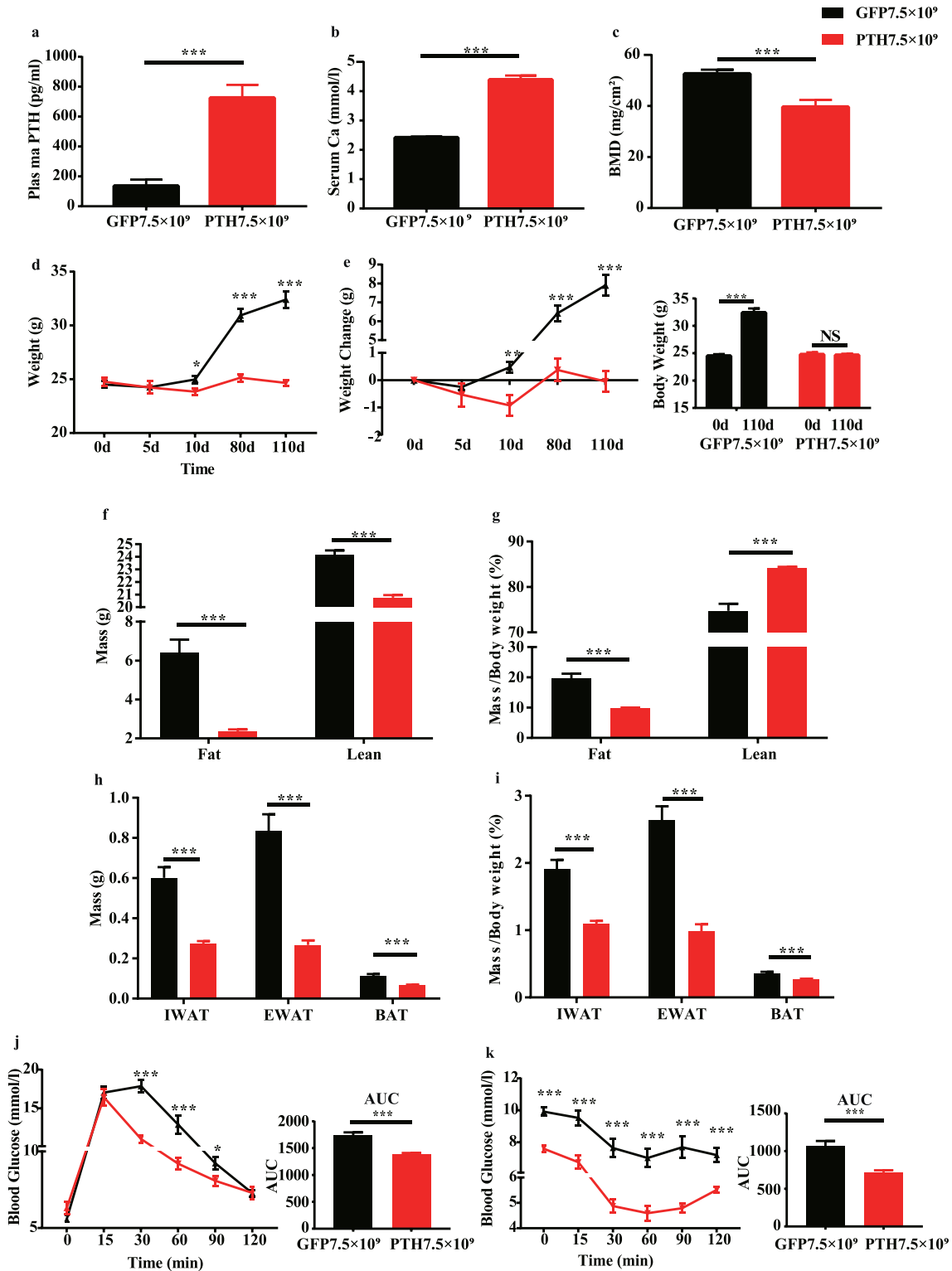
Fig. 1. PHPT mice exhibits reduced body weight, decreased fat content, and improved glucose torerance and insulin sensitivity. (a) The palsma PTH levels of mice 4 months after virus injection. $N = 10$ and 12 in GFP and PHPT group, respectively. (b) The serum calcium 4 months after injection. $N = 8$ in each group. (c) The bone mineral density of distal femur 21 days after virus injection. N = 8 in each group. (d) The body weight of the mice groups followed by virus injection. N = 10 and 12 in GFP and PHPT group, respectively. (e) The changing value of body weight followed by virus injection. N = 10 and 12 in GFP and PHPT group, respectively. For the left panel, independent t-test was performed to make comparisons between GFP and PHPT group. For the right panel, paired t-test was performed to make comparisons between the body weight on 110d and baseline. (f-g) The absolute and relative fat mass and lean mass measured 3.5 months after virus injection. N = 10 and 12 in GFP and PHPT group, respectively. (h) The absolute weight of adipose tissue in mice 4 months after virus injection. N = 10 and 11 in GFP and PHPT group, respectively. (i) The relative adipose tissue weight adjusted by body weight 4 months after virus injection. N = 10 and 12 in GFP and PHPT group, respectively. (j) The intraperitoneal glucose tolerance test performed 3 months after virus injection. N = 10 and 12 in GFP and PHPT group, respectively. (k) The insulin tolerance test performed 3.5 months after virus injection. N = 10 and 12 in GFP and PHPT group, respectively. Data are shown as Means ± SEMs. *$P < .05$, **$P < .01$, ***$P < .001$ vs GFP group.

adrenal disease, cardiovascular disease, or kidney failure; 5) without a body weight change of >5% in the last three months; and 6) with normal serum calcium and phosphorus concentrations.

The ^{18}F-FDG-PET/CT scans (GE DiscoveryTM VCT PET/CT, GE Medical Systems, USA) were performed following a fast for at least eight hours. The ^{18}F-FDG was injected into the vein at a dose of 0.15 mCi/kg body mass (BM), the patient rested for 60 min at room temperature, and then the whole-body PET/CT scan was performed for a total of 30 min. The analysis of the images was performed using Advantage Workstation VolumeShare 2 (GE Medical Systems, USA).

First, the average FDG intake (expressed as the SUV_{mean}) of adipose tissue in each patient was calculated for the following positions: left and right neck, left and right supraclavicular, and paravertebral. The adipose tissue was defined as the region with a Hounsfield Unit range between −10 and −190 on CT scanning. Next, we investigated the presence of

BAT in the subjects using the following criteria: adipose regions with maximum SUV (SUV_{max}) of ≥1.5 were defined as detectable BAT [19]. For the detected BAT region, the SUV_{mean} and SUV_{max} were calculated to investigate the activity of the BAT.

2.16. Study approval

This study protocol was approved by the Ethics Committee of Rui-jin Hospital affiliated to Shanghai Jiao-tong University School of Medicine. All the patients gave informed consent for participating in this study.

2.17. Statistics

For the results of the study in PHPT patients, continuous variables were summarized as means ± SDs or median (interquartile range)
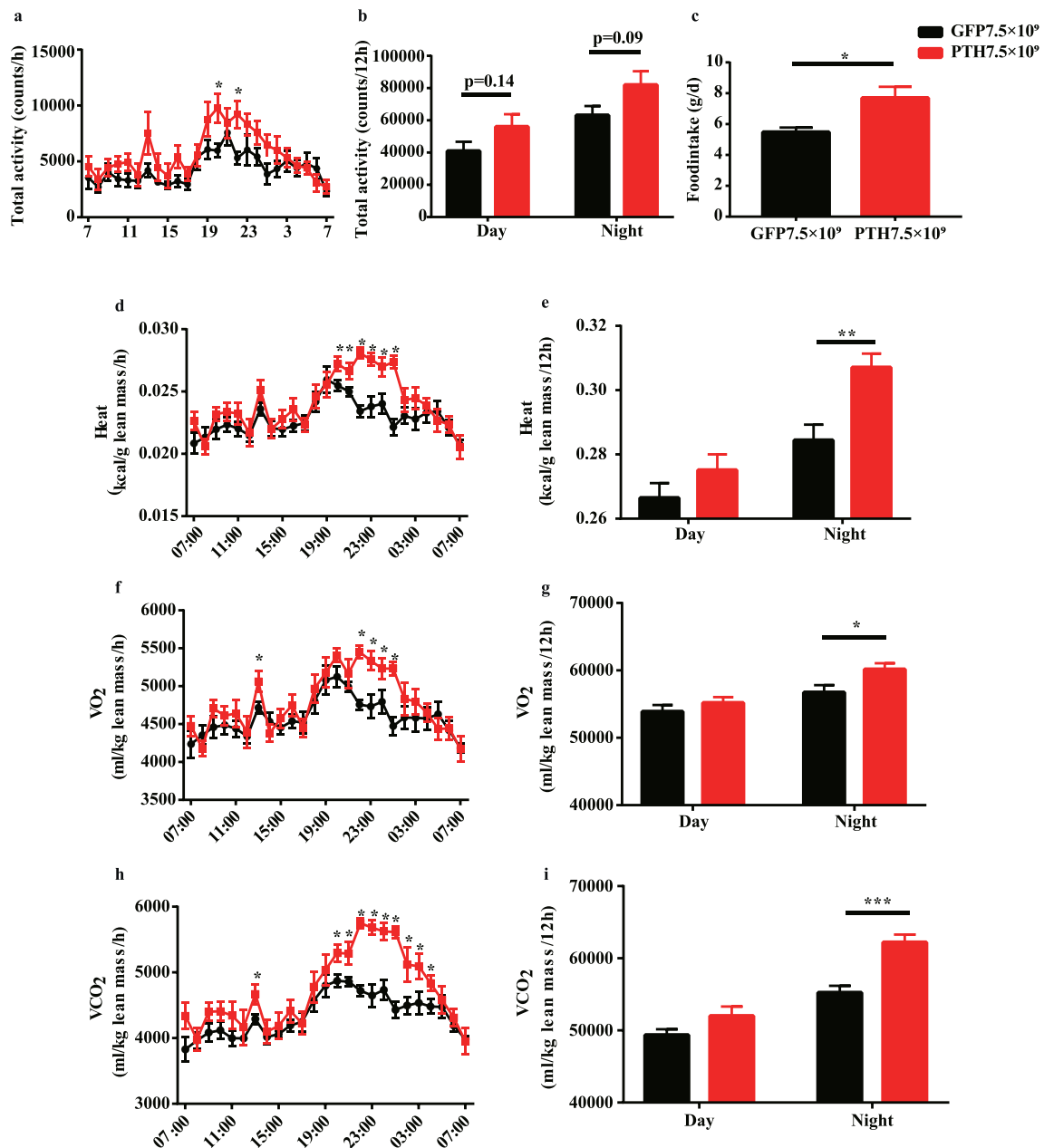

Fig. 2. The energy expenditure is elevated in PHPT mice. The whole-body energy metabolism of PHPT and control mice was measured 3.5 months after virus injection. (a-b) The total activity of every hour or 12 h in mice. (c) The accumulated food intake of 24 h. (d) The average energy expenditure per hour. (e) The accumulated energy expenditure of 12 h. (f) The average O_2 consumption per hour. (g) The accumulated O_2 consumption of 12 h. (h) The average CO_2 production per hour. (i) The accumulated CO2 production of 12 h. Data are shown as Means ± SEMs. N = 8 in each group. *$P < .05$, **$P < .01$, ***$P < .001$ vs GFP group.

according to their distributions, and categorical variables were summarized as number (frequency). The comparisons of measurement data between groups were performed using one-way ANOVA. Chi-square tests were performed to compare the numeration data between groups. General linear regression and multiple linear regression analyses were used to investigate the association between serum PTH levels and
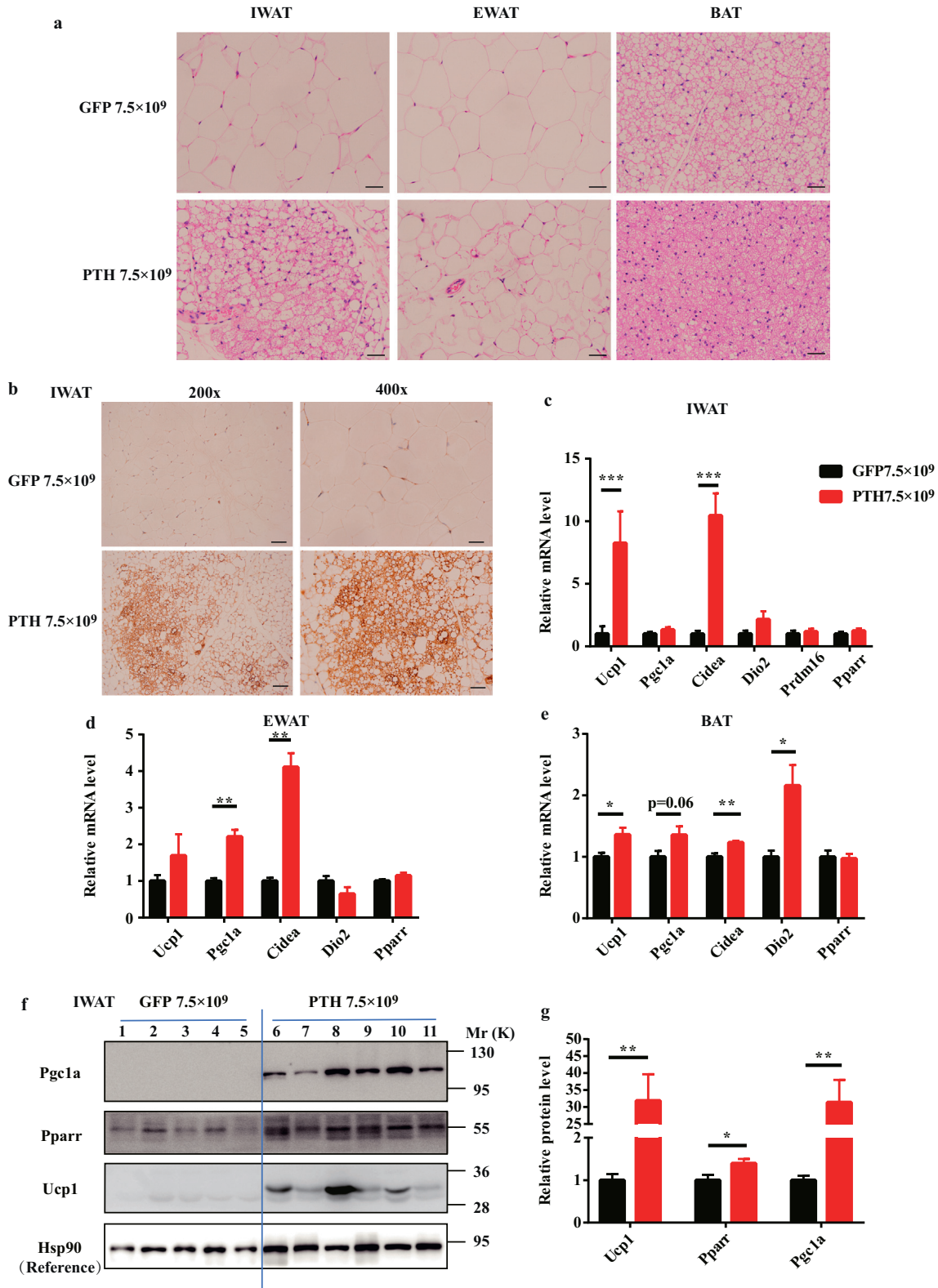

Fig. 3. Excessive secretion of PTH triggers adipose tissue browning in PHPT mice. (a) Representative images of HE staining of adipose tissue sections in mice; scale bar 20 μm. (b) Representative images of the UCP1 staining of IWAT; scale bar, 50 μm for the left panels, and 20 μm for the right panels. (c-e) The relative mRNA level of thermogenic genes in IWAT (c), EWAT (d), BAT (e) of mice. 36b4 is used as the internal reference for normalization. Data are shown as Means ± SEMs; N = 10 and 12 in GFP and PHPT group, respectively. (f) The protein level of thermogenic genes in IWAT measured by western blot. Each lane represents protein sample from one mouse. Lane 1–5 are GFP group and lane 6–11 are PHPT group. Hsp90 is used as the internal reference for normalization. (g) The densitometric analysis of panel f. *$P < .05$, **$P < .01$, ***$P < .001$ *vs* GFP group.

body weight/BMI. For data that were not normally distributed, one-way ANOVA and linear regression analyses were performed after logarithmic transformation. Logistic regression was performed to calculate the odds ratio of low body weight (BMI < 18.5 kg/m^2) per doubling of serum PTH levels relative to its upper normal limit (68.3 pg/ml). For results in mice, data were shown as means±SEMs in figures. The comparisons between groups were made by student t-tests. All statistical calculations were performed using the SAS statistical system (version 8.0; SAS Institute, Cary, NC, USA). A P-value<.05 was considered statistically significant.

3. Results

3.1. Mice model which mimic PHPT exhibits remarked body weight and body fat loss

We first established a mice model which mimicked the biochemical abnormalities of PHPT. We utilized adeno-associated virus (AAV)2/ 9 to overexpress mouse Pth gene to induce sustained PTH secretion. Four months after a single tail-vein injection of the virus, the plasma concentration of mouse PTH 1–84 was significantly increased 4–5 folds (Fig. 1a) in the AAV-PTH group compared to the control group injected with the same dose of empty virus AAV-GFP. Serum calcium levels were concomitantly increased (Fig. 1b) while the bone mineral density was dramatically decreased in mice that received AAV-PTH injections (Fig. 1c), indicating that the mice model successfully simulated the patho-physiological condition of PHPT (hereafter, this mice model will be referred to as PHPT mice for simplicity).

Body weight was not significantly different between the mice groups at baseline. Four months following the virus injection, control mice exhibited gradually weight gain of about 8 g, while the body weight of PHPT mice remained unchanged. Both the body weight and the gaining of weight were much lower in PHPT mice compared with control ones (Fig. 1d and e). Furthermore, fat content was also considerably diminished in PHPT mice no matter it was adjusted by body weight or not (Fig. 1f and g). Concomitantly, both absolute and relative weight of inguinal WAT (IWAT), epididymal WAT (EWAT), and brown adipose tissue (BAT) were decreased in PHPT mice (Fig. 1h and i). In line with the lean phenotype, PHPT mice showed lower fasting blood glucose with improved glucose tolerance (Fig. 1j) and improved insulin sensitivity (Fig. 1k).

3.2. Enhanced energy expenditure in PHPT mice

To investigate whether the body weight loss in PHPT mice was due to a decrease in food intake or an increase in energy expenditure, we did the whole-body energy measurement three and a half months after the virus injection. We found no significant difference in total activity (Fig. 2a and b) between PHPT and control mice. The total food intake of 24 h was even increased in PHPT group (Fig. 2c). Notably, PHPT mice showed higher energy expenditure (Fig. 2d), during night time in particular (Fig. 2e), which was further evidenced by increased O_2 consumption (Fig. 2f and g) and CO_2 production (Fig. 2h and i). Taken together, the over-production of PTH in the PHPT mice reduced body weight and adiposity possibly by elevating the energy expenditure rather than reducing food intake or increasing activity.

3.3. The browning activity of WAT is dramatically induced in PHPT mice

Driven by the hypothesis that the WAT browning contributes to the elevated energy expenditure and decreased body weight in PHPT, we next examined the browning changes of adipose tissue in PHPT mice. In HE staining, compared with the typical WAT with ivory, large, and unilocular adipocytes in the IWAT of control mice, PHPT mice showed "brown like" IWAT with small, multilocular adipocytes (Fig. 3a). Though the "brown-like" tissue was not observed in EWAT of PHPT mice, the adipocytes became much smaller than those in control mice (Fig. 3a). Meanwhile, the histological morphology of BAT in PHPT mice was much denser with smaller drop lipids and more cytoplasm compared with control mice (Fig. 3a). Consistent with these morphological transitions, the brown adipocyte specific marker, uncoupling protein 1 ($Ucp1$), showed remarkable higher positive staining in IWAT of PHPT mice (Fig. 3b). Concomitantly, the mRNA levels of $Ucp1$ and other thermogenic genes, including $Pgc1a$, $Cidea$, and $Dio2$, were increased in IWAT, EWAT, and BAT of PHPT mice (Fig. 3c–e). These molecular alterations were further evidenced by western blot of IWAT which showed a strikingly increased expression of $Ucp1$ and $Pgc1a$ in PHPT mice than the control ones (Fig. 3f and g). These results clearly revealed that long-term excessive secretion of PTH could trigger the WAT browning program.

3.4. Exogenous PTH treatment triggers WAT browning both in vivo and in vitro

To further explore the direct effect of PTH on WAT browning, we treated mice with PTH1–34, an effective fragment of the intact peptide PTH1–84. Two hours after subcutaneous injection, the mRNA levels of thermogenic genes, including $Ucp1$, $Pgc1a$, $Cidea$, and $Dio2$, were dramatically induced in IWAT of PTH injection group compared with the control group (Suppl Fig. 1a), though the similar inducing effect was not observed in EWAT and BAT (Suppl. Fig. 1b–c).

Table 1
The clinical characteristics of PHPT patients at baseline.

PTH	Total	Tertile 1	Tertile 2	Tertile 3	Correlation between PTH and clinical index	
	N = 496	<196 pg/ml	196–465.1 pg/ml	>465.1 pg/ml	β	P
		N = 165	N = 165	N = 166		
Age	54 (46,61.5)	56 (50, 63)	54 (46,62)	51 (41, 59)*	−0.06	<0.0001
Male/Female (%)	145/351 (29.2/70.8)	37/128 (22.4/77.6)	49/116 (29.7/70.3)	59/107 (35.5/64.5)*	/	/
Duration (months)	5 (1,24)	6 (2,36)	4.5 (1,24)	6 (1,24)	−0.07	0.47
Body weight (kg)	60 (52,68)	61 (55,69)	60 (53, 69)	57 (49, 65)*	−0.03	<0.0001
BMI (kg/m^2)	22.4 (20.3,24.9)	22.9 (20.8,25.4)	23.0 (20.6, 25.1)	21.9 (19.3, 24.2)*	−0.04	<0.0001
Calcium (mmol/l)	2.77 (2.56,3.01)	2.57 (2.44,2.70)	2.75 (2.58, 2.92)*	3.11 (2.87,3.36)*	0.08	<0.0001
Phosphorus (mmol/l)	0.84 (0.70,0.99)	0.98 (0.86, 1.09)	0.85 (0.74, 0.94)*	0.72 (0.60, 0.82)*	−0.14	<0.0001
25 (OH)D (nmol/l)	27.0 (15.3, 37.9)	31.5 (17.8,43.8)	26.0 (14.5, 35.5)*	23.3 (14.2, 33.1)*	−0.08	0.02
Scr (μmol/l)	68 (56, 85)	63 (55, 73)	68 (54, 82)	82 (60, 119)*	0.12	<0.0001
Albumin (g/l)	38 (35,40)	38 (36,41)	38 (36,40)	37 (34,40)*	−0.03	<0.0001
BMDL1-4 (g/cm^2)	0.92 (0.79,1.05)	0.98 (0.87,1.09)	0.95 (0.81, 1.07)	0.85 (0.75,1.00)*	−0.08	<0.0001
BMD total hip (g/cm^2)	0.78 (0.68,0.89)	0.83 (0.73,0.94)	0.80 (0.71, 0.89)	0.70 (0.60,0.82)*	−0.11	<0.0001

Values are shown as median (interquartile range) or N (%); Scr: serum creatinine; BMD: Bone mineral density; L1-4: lumbar 1–4.
* P < .05 $vs.$ PTH tertile 1.

Next, to test the cell autonomous effects of PTH on browning, we isolated primary stromal vascular fraction (SVF) from mouse IWAT and treated with rat PTH1-84 during its differentiation into beige adipocytes. Both the mRNA level of *Ucp1* (Suppl Fig. 2a–c) and the oxygen consumption rate (OCR) (Suppl Fig. 2d) was increased in differentiated beige adipocytes treated with PTH1-84, indicating the direct browning-promoting effect of PTH both *in vivo* and *in vitro*.

Taken together, the over-production of PTH in mice which simulating the patho-physiological condition of PHPT induced the WAT browning program, leading to increased energy expenditure, decreased fat content, and finally reduced body weight. These results prompted us to ask whether the elevated serum PTH level could also stimulate brown/beige adipose activity and resulte in body weight loss in humans.

3.5. Serum PTH levels are negatively correlated with body weight and BMI in patients with PHPT

We next investigated the correlation between serum PTH levels and BMI/body weight in a cohort of 496 PHPT patients, whose baseline characteristics are shown in Table 1 according to their PTH tertiles. Of note, both BMI and body weight in the third PTH tertile were significantly lower than those in the first tertile (Table 1). Consistently, general regression analysis showed that serum PTH was negatively correlated with BMI (Fig. 4a) and body weight (Fig. 4b). This correlation remained significant after adjustment of demographic data including age and sex (Table 2, Model 2). Serum albumin and calcium were in correlation with both serum PTH (Table 1) and BMI (Suppl Table 1). After adjustment of these indexes, the association between PTH and BMI/body weight still remained significant (Table 2, Model 3 and 4). Since serum phosphorus, creatinine, 25(OH)D, and the pathological diagnosis (benign/malignancy) were known to be correlated with body weight, they were further selected as confounding factors for the multivariate regression analysis. Still, high serum level of PTH was associated with low BMI/Body weight independent of serum creatinine, phosphorus, 25(OH)D and pathological diagnosis (Table 2, Model 5).

Furthermore, we assessed the prevalence of lean subjects (BMI < 18.5 kg/m^2) in PHPT patients in each PTH tertile and found a significantly increased percentage in the third tertile compared to that in the first tertile ($P = .01$ in χ^2 test, Fig. 4c). A Logistic regression analysis further showed a 5.3% increase in risk of low body weight with every doubling of serum PTH relative to its upper normal limit (68.3 pg/ml) in PHPT patients (Table 3, Model 1). This effect was independent of confounding factors, including age, sex, serum concentrations of albumin, calcium, phosphorus, creatinine, 25(OH)D, and pathological diagnosis (Table 3, Model 2–5).

These data demonstrated that higher serum PTH levels were associated with lower body weight independently of serum calcium levels, renal function, and nutritional index such as albumin in PHPT patients. These findings raised the question whether the adipose tissue browning process contributes to body weight loss in PHPT?

3.6. The brown/beige adipose tissue is functionally activated in PHPT patients

We next retrospectively reviewed the ^{18}F-FDG-PET/CT images from 20 PHPT patients and 60 controls matched for age, sex, and outdoor temperature (clinical characteristics shown in Table 4) to evaluate their brown/beige adipose tissue activities. Using a threshold for activated BAT of SUV$_{max}$ ≥ 1.5 with Hounsfield Unit −10 and − 190 [19], 20% of the PHPT patients (4 out of 20) exhibited detectable activated BAT, which was much higher than the controls with a prevalence of only about 3.3% (2 out of 60) ($P = .03$) (Table 4). Furthermore, the mean standard uptake value (SUV$_{mean}$) was also higher in PHPT patients in cervical (Fig. 5a–b), supraclavicular (Fig. 5c–d), and paravertebral (Fig. 5e) adipose tissue, which have high prevalence of BAT activities and molecular index in humans as identified in previous

studies [19,20]. These data suggested that elevated PTH levels could also increase the metabolic activity of brown/beige adipose tissue in humans, which was in a high accordance with what we observed in PHPT mice.

4. Discussion

In the current study, we found that the elevated serum PTH levels promoted adipose tissue browning, which contributed to body weight loss in PHPT mice and patients.

PTH is a classical calcium-regulating hormone which has long been recognized to act mainly on kidney and bone [1]. Driven by recent

a

R^2=0.0359; β=-0.031
P<0.0001
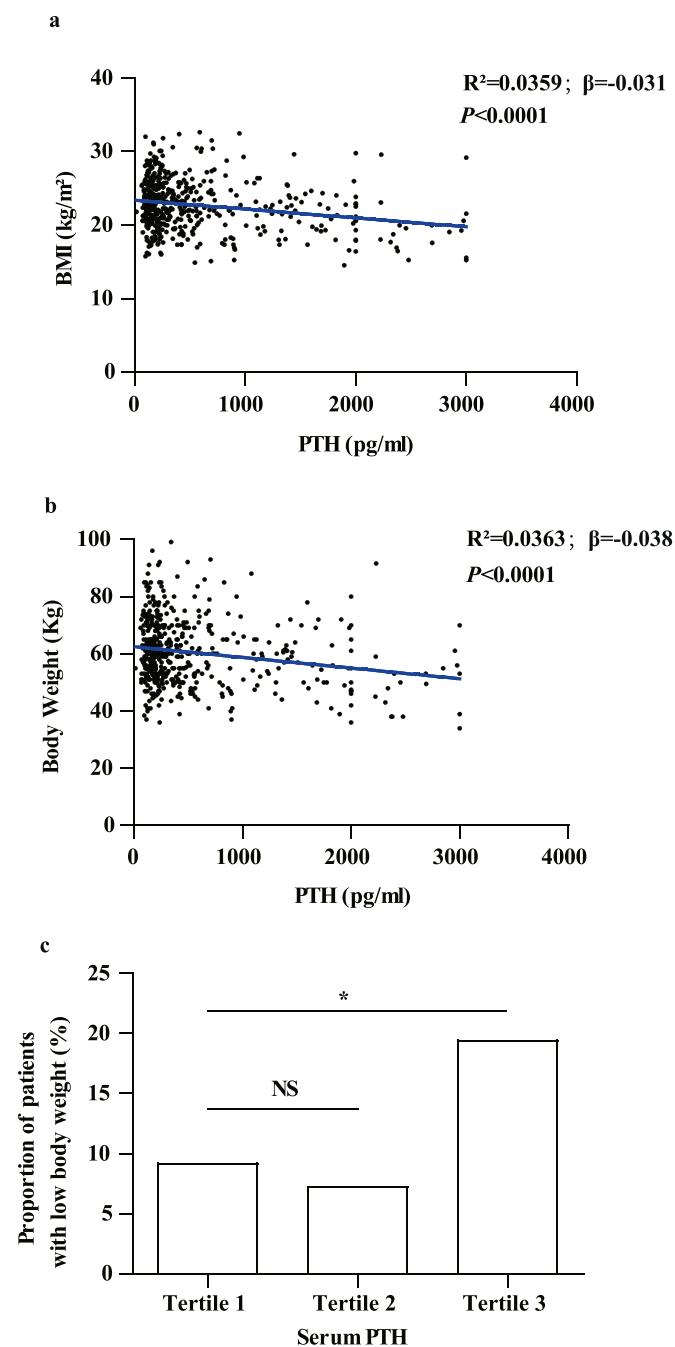
b

R^2=0.0363; β=-0.038
P<0.0001

c

Fig. 4. Serum PTH is negatively associated with BMI or body weight in PHPT patients. (a) The scatter diagram of serum PTH and BMI in PHPT patients. $N = 496$. (b) Scatter diagram of serum PTH and body weight in PHPT patients. N = 496. (c) The proportion of PHPT patients with low body weight (BMI < 18.5 kg/m^2) according to the serum PTH concentration tertiles. *$P < .05$, **$P < .01$, ***$P < .001$.

findings that PTHrP-PTHR pathway promotes WAT browning [3], our current study provided evidence for the notion that adipose tissue is another target organ of PTH, and PTH is an additional hormone facilitating adipose browning activity in addition to the known browning-promoting hormone of thyroid and catecholamine hormones [21].

Consistent with our results from PHPT mice that PTH triggers WAT browning, Kir et al. had reported that renal failure mice with elevated serum PTH (secondary hyperparathyroidism) have increased WAT browning and cachexia which could be blunted by PTHR ablation in adipose tissue [4]. Notably, the PHPT model utilized in our study is more specific in clarifying the effect of PTH than the kidney failure model in the previous study, of which the compensatory PTH secretion is always complicated with other metabolic related confounding factors such as malnutrition, inflammation, and acidosis [22]. Our study provided straightforward *in vivo* and *in vitro* evidence for the browning induction effect of PTH from both PTH excessively secreted model and exogenous PTH treatment model.

The novel pathological effect of PTH on adipose tissue found both in the current and previous study prompted us to make a carefully re-thinking of the patho-physiological changes in PHPT, a common endocrine disorder traditionally characterized by hypercalcemia and its related gastrointestinal, renal, and skeleton manifestations [1].

The activated WAT browning is known to be an energy-consuming program which results in body fat and weight loss [2]. Consistently, the PHPT mice in the current study exhibited remarkable WAT browning, elevated energy consumption, decreased body fat content and reduced body weight. The next important question is how does the browning activity and body weight change in PHPT patients. In the pioneer work of Kir, et al. [4], an increased mRNA levels of thermogenic genes were observed in deep cervical adipose tissue from 12 PHPT patients, however, no metabolic index of these patients or a larger patient population were described. In this study, utilizing a relatively large PHPT cohort, we observed that the risk for low body weight increased by 5.9% with every doubling of serum PTH levels after adjustment of age, sex, serum calcium, phosphorus, creatinine, 25(OH)D, albumin, and pathological diagnosis. Our further study of 20 PHPT patients and matched 60 controls by reviewing their ^{18}FDG-PET/CT data, the most recommended non-invasive method [19] to assess the presence or absence of human brown or beige adipose tissues, revealed that both the prevalence and the metabolic activity of brown/beige adipose tissues were increased in PHPT patients compared with the controls, which partly explained the decreased body weight with higher PTH levels.

The above data indicated a likely high energy consuming condition of PHPT, which provided a new insight in the metabolic changes of the disease. Contrary to our findings, some other human studies reported that PHPT patients showed increased body weight, elevated fat content, and higher prevalence of insulin resistance and metabolic syndrome [12–15]. One likely explanation is the severity of PHPT. In the current study, the decreased body weight was more predominant in the third PTH tertile (>465.1 pg/ml). Meanwhile, both the PHPT patients and

Table 2
The association between PTH and BMI/body weight.

	PTH and BMI (n = 496)			PTH and Body weight (n = 496)		
	β	R²	P	β	R²	P
Model 1	−0.031	0.0359	<0.0001	−0.038	0.0363	<0.0001
Model 2	−0.029	0.0751	<0.0001	−0.046	0.2396	<0.0001
Model 3	−0.026	0.0934	0.0005	−0.042	0.2583	<0.0001
Model 4	−0.029	0.0943	0.005	−0.041	0.2580	0.0004
Model 5	−0.034	0.1224	0.006	−0.048	0.2923	0.0003

Model 1: general regression analysis;
Model 2: adjusted for age, sex;
Model 3: adjusted for age, sex, albumin.
Model 4: adjusted for age, sex, albumin, calcium, phosphorus.
Model 5: adjusted for age, sex, albumin, calcium, phosphorus, 25(OH)D, serum creatinine, pathological diagnosis.

Table 3
The odds ratio for low body weight (BMI < 18.5 kg/m²) with the increased serum level of PTH.

Per doubling of PTH[a] (per 68.3 pg/ml)	OR	95%CI	P
Model 1	1.053	1.028, 1.078	<0.0001
Model 2	1.051	1.026, 1.076	<0.0001
Model 3	1.045	1.018, 1.072	0.001
Model 4	1.041	1.009, 1.074	0.011
Model 5	1.059	1.019, 1.101	0.004

Model 1: univariate logistic regression analysis;
Model 2: adjusted for age, sex;
Model 3: adjusted for age, sex, albumin.
Model 4: adjusted for age, sex, albumin calcium, phosphorus.
Model 5: adjusted for age, sex, albumin, calcium, phosphorus, 25(OH)D, serum creatinine, pathological diagnosis.
[a] The upper normal limit of serum PTH (68.3 pg/ml) is used as one unit to calculate the odds ratio for low body weight per doubling of serum PTH.

mice which showed increased brown/beige adipose activity had high serum PTH of about >1000 and 800 pg/ml respectively. Yet, in other studies which suggested PHPT had higher fat or metabolic syndrome, only asymptomatic or mildly symptomatic PHPT patients were included [13,15]. As a matter of fact, several studies did notice the discrepancies in metabolic index between asymptomatic and symptomatic ones: Procopio et al. [23] found that compared with the controls, metabolic syndrome was more prevalent in only asymptomatic but not in symptomatic PHPT patients. Similarly, Tassone et al. [24] reported that asymptomatic PHPT patients showed higher prevalence of metabolic syndrome than symptomatic ones. In a meta-analysis [25], the degree of hypercalcemia (which largely determined by PTH levels) appeared to have a decisive role in the correlation between body weight and PHPT: when serum calcium was higher than 11.70 mg/dl (2.93 mmol/l), PHPT patients weighed lower than control population, otherwise, PHPT patients had higher body weight. Thus, the discrepancy between the increased body weight or metabolic syndrome reported in PHPT by others and the activated beige/brown adipose tissue in PHPT which leads to body weight loss found in this study might be due to the difference in disease severity or stage. Importantly, results from this study reminded endocrinologists to pay attention to the increased energy-consuming condition in the management of symptomatic PHPT patients, specifically in those with severe condition.

Another point needs to be noted is the reason for weight loss in PHPT. Hypercalcemia and its related gastrointestinal symptoms [1], such as nausea and vomiting, are believed to be responsible for weight loss in PHPT patients. However, when serum albumin, calcium, and other biochemical parameters were adjusted in our PHPT cohort, serum PTH was still inversely associated with the body weight. Furthermore, the food intake in the PHPT mice was even increased which might be explained as a compensatory response to the increased energy expenditure. In accordance with our results, it has been reported that serum PTHrP levels in cancer patients could predict body weight loss

Table 4
Comparisons of clinical characteristics between PHPT patients who had PET/CT Scan and their matched control subjects.

	Control (n = 60)	PHPT (n = 20)	P
Sex(Male/Female)	24/36(40/60)	8/12(40/60)	0.94
Age(yr)	51 (42, 59)	52(41,59)	0.88
BMI(kg/m²)	22.0(20.8,23.7)	21.1(19.0,23.4)	0.87
Outdoor temperature(°C)	19(11.0, 22.5)	17.8(14.0, 23.3)	0.54
Serum calcium(mmol/l)	2.24(2.18,2.29)	3.03(2.83,3.15)	<0.0001
Serum phosphorus(mmol/l)	1.25(1.13, 1.33)	0.68(0.57, 0.81)	<0.0001
Serum PTH(pg/ml)	-*	1369.0 ± 756.2	–
Detectable BAT on PET/CT	2(3.3%)	4(20%)	0.03

* The serum PTH of the control group was unavailable because these control patients were retrospectively selected and their serum PTH were not measured on admission. Data are shown as Means ± SDs, Median (interquartile range), or N(%) according to data distributions.
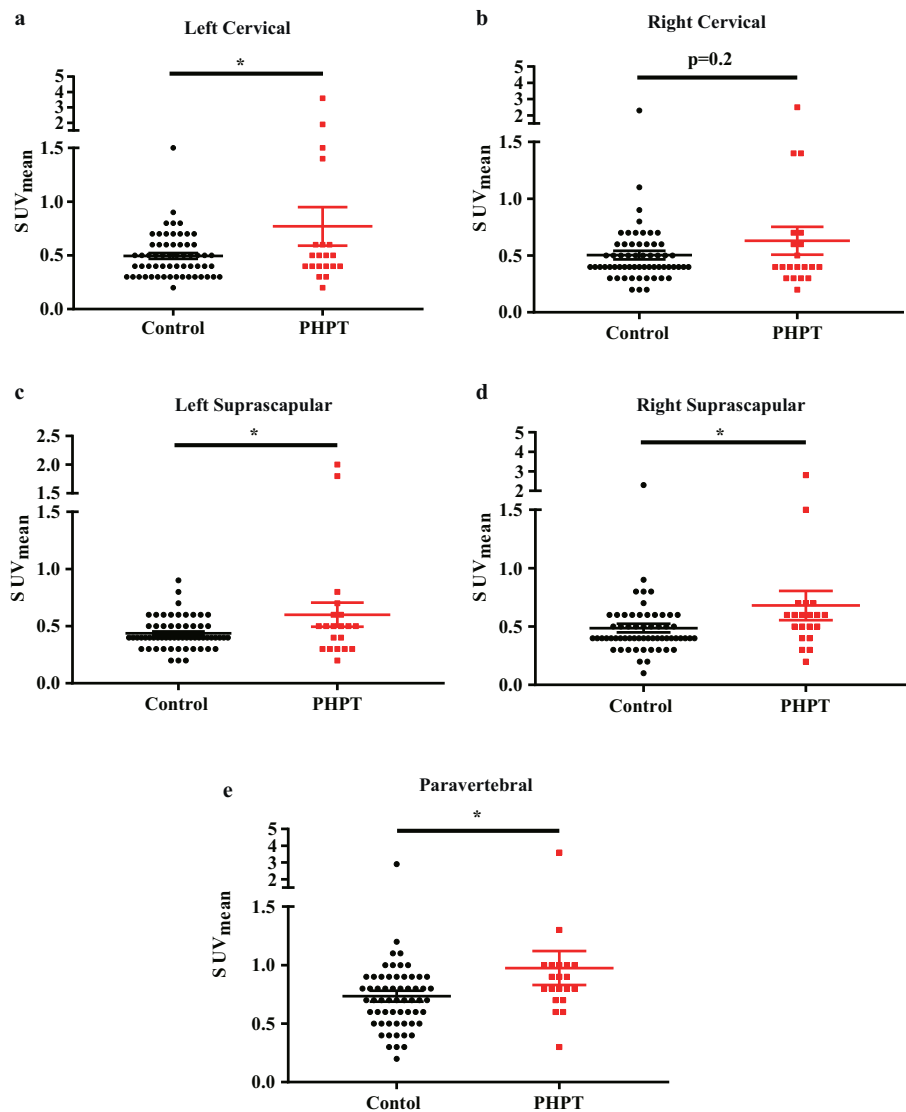
Fig. 5. Brown/beige adipose activity is induced in PHPT patients compared with control ones. Comparisons of SUV$_{mean}$ of adipose tissue between controls and PHPT patients in left cervical (a), right cervical (b), left supraclavicular(c), right supraclavicular (d), and paravertebral (e) regions. $n = 60$ and 20 in controls and PHPT groups, respectively. Data are shown as Means ± SEMs. *$P < .05$, **$P < .01$, ***$P < .001$.

independent of hypercalcemia, serum albumin, and cancer stage [26]. Thus, the weight loss in PHPT could not be simply attributed to hypercalcemia and gastrointestinal symptoms, it is also likely a consequence of increased adipose tissue browning.

Several limitations need to be kept in mind when interpreting findings from the current study. Firstly, we did not utilize the classical PHPT mice model [27], of which the excessive PTH secreted from parathyroid lesions gained by parathyroid targeted over-expression of *cyclin D1* gene [28] or by parathyroid specific deletion of the *Men1* gene [29]. Because the PHPT in these mice was lately onset (>9 months) and the PTH was merely mildly elevated (about 150 pg/ml), which are too aged for the metabolic study in mice and unable to simulated severer condition of PHPT. In the current study, the over-production of PTH of the mice model was gained by *Pth* gene over-expression in AAV infected tissues such as liver, muscle, lung, and heart. Although the hormone source and parathyroid histological changes in the current mice might be different from the classical PHPT models, it successfully simulate the patho-physiological changes of PHPT with elevated serum PTH, calcium, and decreased bone mass, and thus was convincing in investigating the pathological effects of PTH in PHPT. Secondly, since the fat content, which was more closely related with adverse metabolic profiles than

body weight [30], and metabolic rate were not measured in our PHPT cohort, much work remained to be done to explore how and to what extent the increased brown/beige activity affects the energy metabolism and fat mass in PHPT patients.

In conclusion, our findings support the notion that elevated circulating PTH levels drive the WAT browning program, which contributes, in part at least, to the reduced body weight in PHPT mice and patients. These findings provide further evidence for the novel function of a classical hormone, PTH, in body weight regulation and an important insight in understanding the metabolic changes in PHPT.

Conflict of interest

No potential conflicts of interest relevant to this article were reported.

Author contributions

J.W, and J.L conceived the project and designed the experiment. Y·H carried out most of the experiment. Z.Z, N·C, C·S, J.X, X.G, Y.L assisted in some of the experiment. Y·H, M.Z, B.T, H.Z, and L.S recruited primary hyperparathyroidism patients. W·S, R.G, and B.L reviewed the PET-CT data and re-analyzed the SUV of adipose tissue. Y·H and R.L wrote the manuscript. S.L and R.L interpreted the data and contributed valuable comments. G.N, J.W, and J.L were the guarantors of this work and, as such, had full access to all the data in the study and take responsibility for the integrity of the data and the accuracy of the data analysis.

Appendix A. Supplementary data

Supplementary data to this article can be found online at https://doi.org/10.1016/j.ebiom.2018.11.057.

References

[1] Bilezikian JP, Cusano NE, Khan AA, Liu JM, Marcocci C, Bandeira F. Primary hyperparathyroidism. Nature Reviews Disease Primers 2016;2:16033.

[2] Abdullahi A, Jeschke MG. White adipose tissue browning: A double-edged sword. Trends Endocrinol Metab 2016;27:542–52.

[3] Kir S, White JP, Kleiner S, Kazak L, Cohen P, Baracos VE, et al. Tumor-derived PTH-related protein triggers adipose tissue browning and cancer cachexia. Nature 2014;513:100–4.

[4] Kir S, Komaba H, Garcia AP, Economopoulos KP, Liu W, Lanske B, et al. PTH/PTHrP receptor mediates cachexia in models of kidney failure and cancer. Cell Metab 2016;23:315–23.

[5] McCauley LK, Martin TJ. Twenty -five years of PTHrP progress: from cancer hormone to multifunctional cytokine. J Bone Miner Res 2012;27:1231–9.

[6] Cheloha RW, Gellman SH, Vilardaga JP, Gardella TJ. PTH receptor-1 signalling-mechanistic insights and therapeutic prospects. Nat Rev Endocrinol 2015;11:712–24.

[7] Vilardaga JP, Gardella TJ, Wehbi VL, Feinstein TN. Non-canonical signaling of the PTH receptor. Trends Pharmacol Sci 2012;33:423–31.

[8] Karaplis AC, Luz A, Glowacki J, Bronson RT, Tybulewicz VL, Kronenberg HM, et al. Lethal skeletal dysplasia from targeted disruption of the parathyroid hormone-related peptide gene. Genes Dev 1994;8:277–89.

[9] Miao D, He B, Karaplis AC, Goltzman D. Parathyroid hormone is essential for normal fetal bone formation. J Clin Investig 2002;109:1173–82.

[10] Clines GA. Mechanisms and treatment of hypercalcemia of malignancy. Curr Opin Endocrinol Diabetes Obes 2011;18:339–46.

[11] Nakayama K, Fukumoto S, Takeda S, Takeuchi Y, Ishikawa T, Miura M, et al. Differences in bone and vitamin D metabolism between primary hyperparathyroidism and malignancy-associated hypercalcemia. J Clin Endocrinol Metab 1996;81:607–11.

[12] Corbetta S, Mantovani G, Spada A. Metabolic syndrome in parathyroid diseases. Front Horm Res 2018;49:67–84.

[13] Kamycheva E, Sundsfjord J, Jorde R. Serum parathyroid hormone level is associated with body mass index. The 5th Tromsø study. Eur J Endocrinol 2004;151:167–72.

[14] Di Monaco M, Castiglioni C, Vallero F, Di Monaco R, Tappero R. Parathyroid hormone is significantly associated with body fat compartment in men but not in women following a hip fracture. Aging Clin Exp Res 2013;25:371–6.

[15] Mendoza-Zubieta V, Gonzalez-Villaseñor GA, Vargas-Ortega G, Gonzalez B, Ramirez-Renteria C, Mercado M, et al. High prevalence of metabolic syndrome in a mestizo group of adult patients with primary hyperparathyroidism (PHPT). BMC Endocr Disord 2015;15:16.

[16] Wang J, Liu R, Wang F, Hong J, Li X, Chen M, et al. Ablation of LGR4 promotes energy expenditure by driving white-to-brown fat switch. Nat Cell Biol 2013;15:1455–63.

[17] Liu M, Zhang X, Li A, Zhang X, Wang B, Li B, et al. Insulin treatment restores islet microvascular vasomotion function in diabetic mice. J Diabetes 2017;9:958–71.

[18] Zou Y, Lu P, Shi J, Liu W, Yang M, Zhao S, et al. IRX3 promotes the browning of white adipocytes and its rare variants are associated with human obesity risk. EBioMedicine 2017;24:64–75.

[19] Chen KY, Cypess AM, Laughlin MR, Haft CR, Hu HH, Bredella MA, et al. Brown adipose reporting criteria in imaging studies (BARCIST 1.0): Recommendations for standardized FDG-PET/CT experiments in Humans. Cell Metab 2016;4:210–22.

[20] Cypess AM, White AP, Vernochet C, Schulz TJ, Xue R, Sass CA, et al. Anatomical localization, gene expression profiling and functional characterization of adult human neck brown fat. Nat Med 2013;19:635–9.

[21] Cypess AM, Weiner LS, Roberts-Toler C, Franquet Elía E, Kessler SH, Kahn PA, et al. Activation of human brown adipose tissue by a β3-adrenergic receptor agonist. Cell Metab 2015;21:33–8.

[22] Obi Y, Qader H, Kovesdy CP, Kalantar-Zadeh K. Latest consensus and update on protein-energy wasting in chronic kidney disease. Curr Opin Clin Nutr Metab Care 2015;18:254–62.

[23] Procopio M, Barale M, Bertaina S, Sigrist S, Mazzetti R, Loiacono M, et al. Cardiovascular risk and metabolic syndrome in primary hyperparathyroidism and their correlation to different clinical forms. Endocrine 2014;47:581–9.

[24] Tassone F, Gianotti L, Baffoni C, Cesario F, Magro G, Pellegrino M, et al. Prevalence and characteristics of metabolic syndrome in primary hyperparathyroidism. J Endocrinol Investig 2012;35:841–6.

[25] Bolland MJ, Grey AB, Gamble GD, Reid IR. Association between primary hyperparathyroidism and increased body weight: a meta-analysis. J Clin Endocrinol Metab 2005;90:1525–30.

[26] Hong Namki, Yoon Hye-jin, Lee Yong-ho, Kim Hye Ryun, Lee Byung Wan, Rhee Yumie, et al. Serum PTHrP predicts weight loss in cancer patients independent of hypercalcemia, inflammation, and tumor burden. J Clin Endocrinol Metab 2016; 101:1207–14.

[27] Imanishi Y, Inaba M, Kawata T, Nishizawa Y. Animal models of hyperfunctioning parathyroid diseases for drug development. Expert Opin Drug Discovery 2009;4:727–40.

[28] Imanishi Y, Hosokawa Y, Yoshimoto K, Schipani E, Mallya S, Papanikolaou A, et al. Primary hyperparathyroidism caused by parathyroid-targeted overexpression of cyclin D1 in transgenic mice. J Clin Invest 2001;107:1093–102.

[29] Libutti SK, Crabtree JS, Lorang D, Burns AL, Mazzanti C, Hewitt SM, et al. Parathyroid gland-specific deletion of the mouse Men1 gene results in parathyroid neoplasia and hypercalcemic hyperparathyroidism. Cancer Res 2003;63:8022–8.

[30] Lv X, Zhou W, Sun J, Lin R, Ding L, Xu M, et al. Visceral adiposity is significantly associated with type 2 diabetes in middle-aged and elderly Chinese women: a cross-sectional study. J Diabetes 2017;9:920–8.